Agricultural and Forest Meteorology 285–286 (2020) 107929

Contents lists available at ScienceDirect

Agricultural and Forest Meteorology

journal homepage: www.elsevier.com/locate/agrformet

Oxygen stable isotopes of a network of shrubs and trees as high-resolution plaeoclimatic proxies in Northwestern China

Qiang Li[a,b,c,*], Yu Liu[a,b,c,d,*], Takeshi Nakatsuka[e], Qi-Bin Zhang[f], Keiko Ohnishi[g], Akiko Sakai[e], Osamu Kobayashi[h], Yingnan Pan[i], Huiming Song[a,b,c], Ruoshi Liu[d], Changfeng Sun[a,b,c], Congxi Fang[a,b,c]

[a] State Key Laboratory of Loess and Quaternary Geology, Institute of Earth Environment, Chinese Academy of Sciences, Xi'an 710061, China
[b] CAS Center for Excellence in Quaternary Science and Global Change, Xi'an 710061, China
[c] Interdisciplinary Research Center of Earth Science Frontier (IRCESF) and Joint Center for Global Change Studies (JCGCS), Beijing Normal University, Beijing 100875, China
[d] School of Human Settlements and Civil Engineering, Xi'an Jiaotong University, Xi'an 710049, China
[e] Graduate School of Environmental Studies, Nagoya University, Nagoya 464-8601, Japan
[f] State Key Laboratory of Vegetation and Environmental Change, Institute of Botany, Chinese Academy of Sciences, Beijing, China
[g] Institute of Low Temperature Sciences, Hokkaido University, Sapporo 060-0819, Japan
[h] Institute for International Relations, Ehime University, Ehime 790-8577, Japan
[i] School of Humanities and Arts, Xidian University, Xi'an 710071, China

A B S T R A C T

Tree rings play an important role in high-resolution paleoclimate reconstruction over large areas. Nevertheless, the sampling sites of most existing tree-ring networks are unevenly distributed due to the limitations of the availability of appropriate tree species and sampling conditions. In light of the good spatial representation provided by tree-ring stable oxygen isotope ratio ($\delta^{18}O$), we selected several shrubs (*Hippophae rhamnoides* L.) found in near-glacier valleys, conifer (*Picea crassifolia* Komarov) trees in alpine meadows, and broad-leaved (*Populus euphratica* Olivier) trees found in deserts. Although the three sampling sites were each 250–360 km apart, with varied site conditions and very distinct species, we observed coherent variations in the $\delta^{18}O$ of the three species within a common time interval. The average correlation coefficient was found to be 0.674 ($p < 0.001$, $n = 30$) among annual-ring $\delta^{18}O$ series of three species. All annual-ring $\delta^{18}O$ of three species demonstrated significant negative correlations with relative humidity (RH) and precipitation, and significant positive correlations with temperature, in spring and summer. The correlation coefficient between the first principal component (PC1) of the $\delta^{18}O$ variations in the three species and the regional summer (June to August) RH was found to be -0.855 ($p < 0.001$, $n = 30$). In addition, PC1 showed variations similar to those of $\delta^{18}O$ in precipitation. Spatial correlation demonstrated that PC1 represents the hydroclimatic variability that occurs in most of central-western China. Significant correlations with sea-level pressure and several East Asian Summer Monsoon indices indicated that PC1 was affected by the large-scale atmospheric circulation pattern and could be used as an indicator of monsoon moisture. PC1 correlated significantly with ten annually resolved hydroclimatic series in central-western China, demonstrating the potential of establishing a tree-ring climate network with uniform spatial distribution using multi-species tree-ring $\delta^{18}O$. The results from these series suggest that an abrupt climate change occurred in 1979. After 1979, PC1 correlated significantly with the summer-season EI Nino Modoki index ($r = 0.474$, $p < 0.02$, $n = 24$). This implied that the effect of the central Pacific ENSO on the variability in monsoon moisture in China became more prominent after the abrupt climate change in 1979.

1. Introduction

Tree rings have become very important indicators for studying past climate change due to their high resolution, accurate chronology, and wide distribution. The extraction of common signals from samples at multiple sampling sites in a region for the establishment of regional tree-ring networks has become a feasible route for high-resolution investigation of climate change. For example, a regional Palmer Drought Severity Index (PDSI) series was reconstructed using hundreds of tree-ring width series distributed over North America (Cook et al., 2010b). The Monsoon Asia Drought Atlas (MADA) PDSI Dataset was subsequently constructed using the same method (Cook et al., 2010a). The Eastern Australia and New Zealand Drought Atlas (ANZDA) PDSI Dataset was established using 176 tree-ring width series in eastern Australia and New Zealand (Palmer et al., 2015). In Mongolia, the regional summer PDSI variabilities were reconstructed for the interval 1520–1993 using 34 tree-ring width series (Davi et al., 2010). By combining 53 tree-ring width series and 31 maximum latewood density

* Corresponding authors at: State Key Laboratory of Loess and Quaternary Geology, Institute of Earth Environment, Chinese Academy of Sciences, Xi'an 710061, China
E-mail addresses: liqiang@ieecas.cn (Q. Li), liuyu@loess.llqg.ac.cn (Y. Liu).

https://doi.org/10.1016/j.agrformet.2020.107929
Received 15 June 2019; Received in revised form 24 January 2020; Accepted 2 February 2020
Available online 12 February 2020
0168-1923/

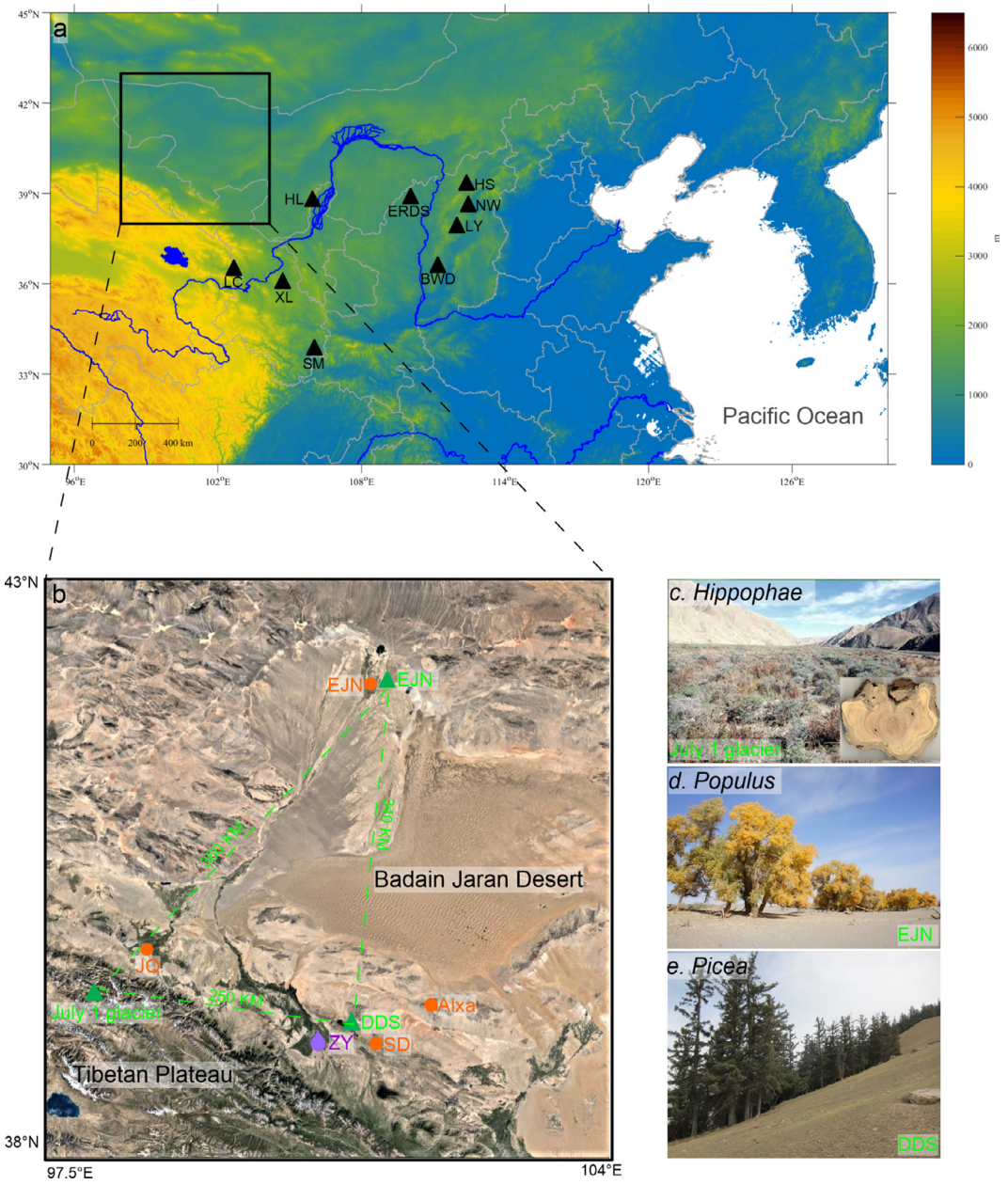

Fig. 1. Map showing the study area (blank rectangle) and locations of contrastive tree-ring based climate constructions (solid triangles) (a), satellite image of the study area (gree triangles indicate the sampling sites; orange circles indicates the meteorological stations; purple drop shows observed station in $\delta^{18}O$ of precipitation in Zhangye; the distance between each sampling site is shown as dashed green line) (b) and the images of sampling sites for *H. rhamnoides* (c), *P. euphratica* (d), *P. crassifolia*(e). (For interpretation of the references to color in this figure legend, the reader is referred to the web version of this article.)

data from the European Alps, the potential for a broad-scale regional climatic reconstruction was demonstrated (Frank and Esper, 2005). Using tree-ring stable carbon ($\delta^{13}C$) and oxygen ($\delta^{18}O$) isotopes from 23 sites across Europe, the first European network of tree-ring isotopes was established, suggesting that tree-ring isotopes, especially tree-ring $\delta^{18}O$, should be a good proxy for use in future establishment of a European climate network (Treydte et al., 2007).

The above studies have made notable contributions to the understanding of broad-scale climate change with high resolution. Nevertheless, we identified the following problems from these studies. Limited conifer tree species and a few broad-leaved tree species (e.g., oak and teak trees) have been used in traditional dendroclimatology (Grissino-Mayer, 1993) . Moreover, there are no tree species suitable for traditional dendroclimatological studies in certain types of landforms (such as deserts and grasslands). Therefore, the problem of uneven spatial distribution of sampling sites arose in most tree-ring networks (Li et al., 2015a; Yang et al., 2013). Because tree-ring width and density are subject to prominent growth-related trends (juvenile effect), which have to be eliminated when establishing the chronologies, the signals of the long-term climate trends could be weakened (Briffa et al., 1996). Tree-ring $\delta^{18}O$ is the ratio between ^{18}O and ^{16}O, which is not related to growth. Thus, detrending is not required in tree-ring $\delta^{18}O$ chronologies. Moreover, the physiological mechanism of tree-ring $\delta^{18}O$ is known from many previous studies. Trees absorb water from soil through their roots. The water is then transported to the leaves to participate in photosynthesis, carbohydrate production, and finally, cellulose synthesis. During these processes, isotope fractionation occurs in the leaves (Song et al., 2014). Due to transpiration, the isotope fractionation in leaves is related to the external relative humidity. As a result, tree-ring $\delta^{18}O$ is determined theoretically, by soil moisture $\delta^{18}O$ (in most places,

the soil moisture is derived from precipitation during the growing season) and external relative humidity (Roden et al., 2000). Hence, in theory, the same trend in $\delta^{18}O$ should be observed in different tree species from the same region. For instance, $\delta^{18}O$ variations were found to be the most consistent among three species that were growing 30 km apart in the North China Plain, including *Pinus tabuliformis* Carriere on the mountain ridge, and *Larix principis-rupprechtii* Mayr and *Picea koraiensis* Nakaiin the alpine meadows (Li et al., 2011c). $\delta^{18}O$ of these species mainly respond to summer precipitation. Coherent changes of $\delta^{18}O$ were observed in *Pinus densiflora* Siebold et Zuccarini, and in *Quercus serrata* Murray that grew in the same forest in central Japan, both responding to relative humidity in summer (Li et al., 2015b). Good coherence of tree-ring $\delta^{18}O$ variation from seven lowland and one highland tree species was found in Bolivia, which could be used to carry out isotopic cross dating (Baker et al., 2015).

The above studies revealed that tree-ring $\delta^{18}O$ can be used as a good proxy in the research on broad-scale dendroclimatic networks. Nevertheless, the growth rings of shrubs were not included in these studies. Shrubs are commonly found in a variety of environments (including deserts, tropics, and subtropics), and have a relatively wide geographical distribution (Lawrence and Hawthorne, 2006). If shrubs were included in future tree-ring network research, we would be able to obtain paleoclimate networks with higher spatial resolution. Hence, more stringent investigations are still required in research related to plant annual ring $\delta^{18}O$ to examine the potential of constructing a future broad-scale plant annual ring $\delta^{18}O$ network with a uniform spatial distribution. Due to widely distribution of shrubs, annual ring $\delta^{18}O$ of shrubs could be potential to reduce uniform spatial distribution of tree-ring network.

In this study, we examined the $\delta^{18}O$ variability in shrubs, conifer trees and broad-leaved trees that were relatively far apart (250–360 km), and these were sampled in various landforms (e.g., near-glacier valleys, alpine meadows, and deserts). We then analyzed the similarities and differences of the variations among different species, as well as the causes for them. The first principal component of $\delta^{18}O$ variations from three species was compared with ten paleoclimate reconstructions over central-eastern China and several East Asian Summer Monsoon indices. Finally, the effect of remote oceans on the $\delta^{18}O$ variation was investigated to enable discussion of possible forcing of large-scale atmospheric circulations.

2. Materials and methods

2.1. Study area and sampling

For this study, we chose three types of plants in northwest China, the sampling sites of which were about 250–360 km apart (Fig. 1). They belong to three different species and grow in different environments at distinct elevations.

The samples of conifer trees (*Picea crassifolia* Komarov) were collected from the upper forest limit of Dongdashan Mountain (DDS in Fig. 1) in the Hexi Corridor in August 2012 (39.1° N, 100.7° E, 2900–3200 m asl). A set of tree-ring core samples was obtained from the trees at breast height using 5 mm increment borers. The sampling site was in the alpine meadows on the northeast slope of Dongdashan Mountain, where *P. crassifolia* is sparsely distributed. This species is a shallow-rooted plant distributed across the Qilian Mountains, Qinghai, Gansu, Ningxia, and Inner Mongolia (mountain areas in northwest China) at elevations of 1000–4000 m asl (Li et al., 2019).

The broad-leaved tree, *Populus euphratica* Olivier is the most ancient poplar tree species in the world (Browicz, 1977). It is a plant from the Tertiary era and a deciduous tree that belongs to the family Salicaceae (Browicz, 1977). It is one of a limited number of tree species that can survive in deserts due to its ability to endure the aridity there (Tang et al., 2013). Moreover, it is tolerant of salinity and has a root depth of 6–8 m (Rajput et al., 2016). It is mainly distributed over extremely arid deserts and along the rivers in central Asia and northwest China (Tang et al., 2013). We collected a set of *P. euphratica* samples from the desert at the edge of Ejina Oasis (42.0° N, 101.1° E, 923 m asl) in October 2011 using 12 mm increment borers.

Hippophae rhamnoides L. is a deciduous shrub that is drought- and sandstorm-tolerant and can survive in saline soils; hence, it is widely planted in arid and semi-arid regions as an anti-sandstorm plant. *H. rhamnoides* could grow more than a hundred years (Zhu et al., 2013). It is mainly distributed in Eurasia from 2 to 115° E and 27 to 68° N. In summer 2004, samples of *H. rhamnoides* were collected in a valley close to the July 1 Glacier (39.6° N, 97.7° E, 3253 m asl).

Cross-dating was conducted using standard methods on the *P. crassifolia* and *P. euphratica* samples after they were brought to the laboratory (Li et al., 2019; Liu et al., 2010, 2012). With regards to *H. rhamnoides*, the total number of rings were fewer and there were fewer samples available. The sampling site of *H. rhamnoides* is within limit of the National Reserve, where vegetation is scarce, and soil is desertificated. Because *H. rhamnoides* growing in the sampling site is low and has many branches, we could not take sample by increment borer. As an important sand-fixation plant, we got the permit that only three *H. rhamnoides* trees could be cut for purpose of scientific research. Several studies have demonstrated that tree-ring isotopes could be potential tools for dating independent with traditional cross dating based on a group of tree-ring width series, which mainly because of high coherence of tree-ring isotopes series within a site (Kagawa and Leavitt, 2010; Leavitt et al., 1985; Loader et al., 2019; Miles et al., 2019; Roden, 2008) Therefore, we compared the tree-ring widths and $\delta^{18}O$ variations of the three disk-samples, but did not undertake systematic cross-dating for the *H. rhamnoides* samples. We finally chose an interval common to the three species (1974–2003) for further analyses.

2.2. Tree-ring $\delta^{18}O$ data

Because we had only three *H. rhamnoides* samples, we selected three tree-ring core samples each of *P. crassifolia* and *P. euphratica* to conduct comparable $\delta^{18}O$ analyses for this study. In order to evaluate whether the $\delta^{18}O$ series of three trees have enough representative in the sampling site, we calculated Expressed Population Signal (EPS) according to the following equation (Wigley et al., 1984):

$$EPS = (n*r_{mean})/[1 + (n - 1)*r_{mean}]$$

Where n is the number of time series, and r_{mean} is mean inter-series correlation (or Rbar).

The annual rings of the selected cores were clear. The selection criteria were that samples should not have missing rings, false rings, or extremely narrow rings. Annual rings were carefully cut into thin sections with a razor blade under a binocular microscope. The boundary between earlywood and latewood was indistinct, which only permitted the separation of whole annual rings. Among wood components, α-cellulose is a very stable natural biopolymer, which does not exchange stable carbon and oxygen isotopes after initial fixation of the light elements (Leavitt, 2010). The α-cellulose in the thin sections of annual rings was extracted using a modified Jayme-Wise method (Li et al., 2017; Loader et al., 1997). Briefly, we used organic reagents, mixed solution of sodium chlorite and acetic acid, and 17.5% solution of sodium hydroxide to perform for removing extractions (resin, ash, and so on), lignin and hemi-cellulose, respectively. We homogenized α-cellulose of annual-ring material using an ultrasonic cell disruptor. Approximately 0.13–0.17 mg of homogeneous α-cellulose was loaded into a silver capsule. The stable oxygen isotope ratio was determined with a pyrolysis-type elemental analyzer (ThermoFisher TC/EA) and an isotope ratio mass spectrometer (ThermoFisher Delta V Advantage). To maintain the independence of measurements, α-cellulose samples of the three species were measured at the Research Institute of Humanity and Nature (Kyoto, Japan), at the Tree-Ring Laboratory in the Institute of Earth Environment, Chinese Academy of Sciences (Xi'an, China), and at

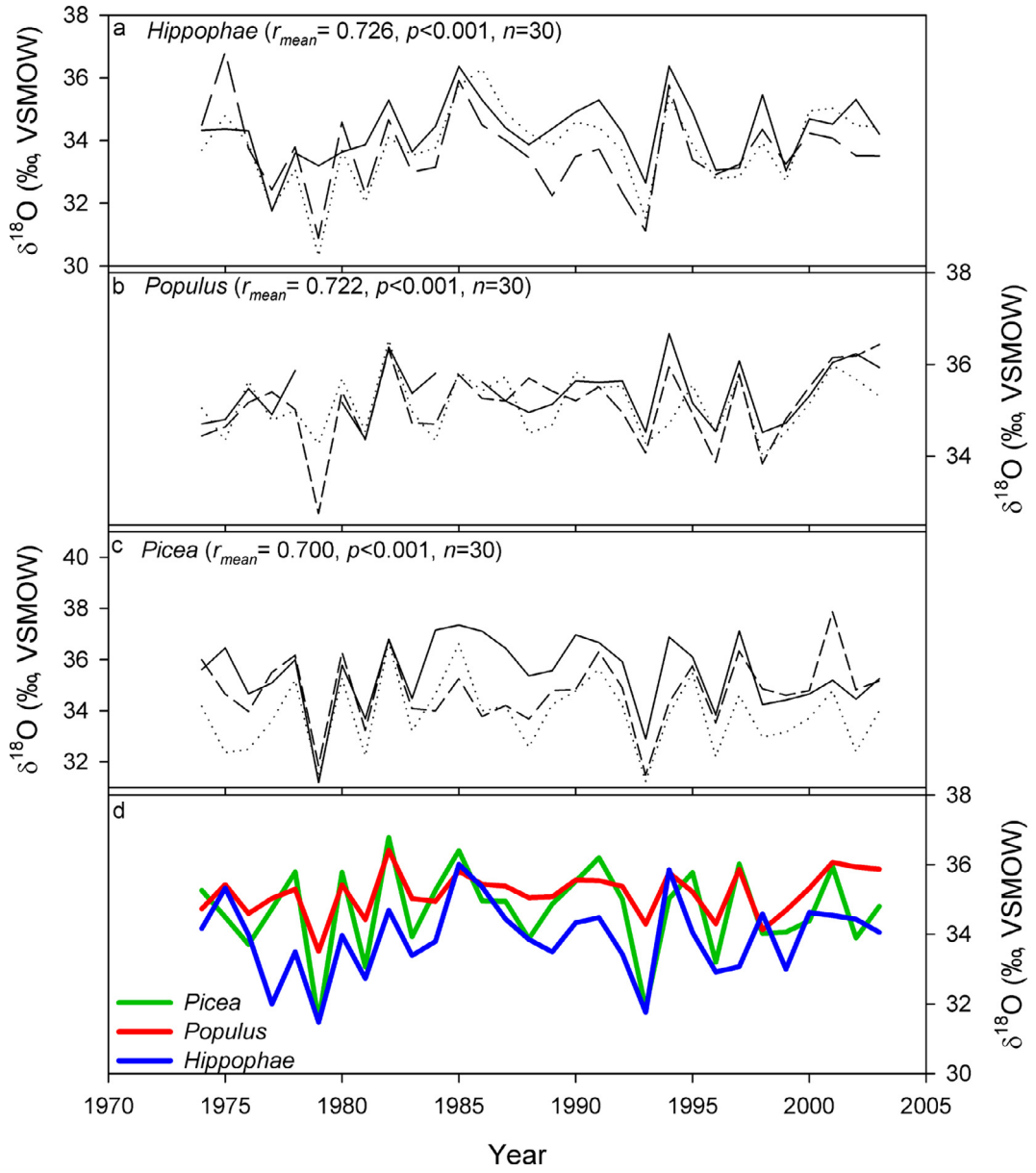

Fig. 2. Individual $\delta^{18}O$ series of *H. rhamnoides* (a), *P. euphratica* (b), *P. crassifolia*(c) and arithmetic averaged $\delta^{18}O$ series of three species (d).

the Institute of Low Temperature Science, Hokkaido University (Sapporo, Japan). Tree-ring stable oxygen isotope ratios were calculated by comparison with an isotope ratio that was predetermined using a commercial cellulose standard (Merck cellulose, Darmstadt, Germany). The Merck cellulose was inserted every eight samples during the measurement process. The oxygen isotope ratios were expressed as $\delta^{18}O$, which represents the permil deviation relative to Vienna Standard Mean Ocean Water (VSMOW). The analytical uncertainty of the repeated measurement of the commercial cellulose was 0.2‰ (1σ).

2.3. Climate data

We adopted climate records from the meteorological stations nearest to the sampling sites of the three species. All the meteorological data used were from the National Meteorological Information Center (https://data.cma.cn). During the instrumental observation, the mean annual precipitation (P) at the meteorological station near the *P. crassifolia* site was 158 mm, more than 60% of which fell in summer (June to August, JJA). The annual mean temperature (T) was 7.68 °C, with the hottest monthly mean temperature in July (22.36 °C) and the coldest monthly mean temperature in January (−9.01 °C). Two peaks in relative humidity (RH) occurred, one in winter and the other in summer. During the growing season of *P. crassifolia* (April to October), the meteorological records show that the long-term RH trend was a slight decrease (−0.033% per year), whereas P and T exhibited trends of increase (0.467 mm/year and 0.025 °C/year, respectively). The meteorological station (Ejina: EJN) near the sampling site of *P. euphratica* is in one of the most arid areas in China. The instrumental observations at EJN revealed a mean annual P of 35 mm, 62% of which fell in summer (JJA). The annual mean T was 9 °C, with the hottest record in July (27 °C) and the coldest in December (−10 °C). The mean annual RH was 34%. The meteorological station nearest the *H. rhamnoides* site was in Jiuquan. There, the mean annual P was 88 mm, 58% of which fell in summer (JJA, June to August). The annual mean T was 7.5 °C, and the mean annual RH was 48%.

We assessed the spatial representativeness of the first principal component (PC1) of the $\delta^{18}O$ variations in the three species from the three sampling sites using global hydroclimatic grid-point datasets. The grid-point datasets consisted of the observed relative humidity (Station RHMEAN), the observed precipitation (Station PR), the mean relative

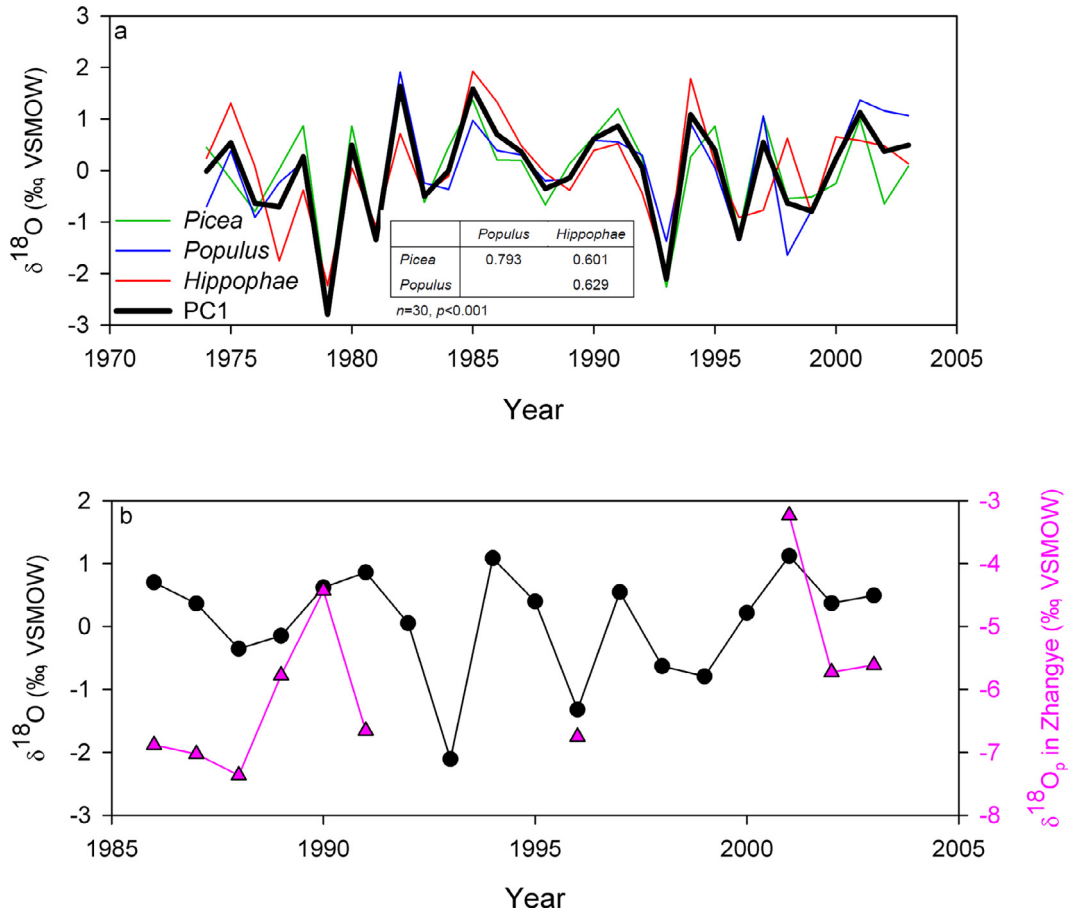

Fig. 3. Standarized mean $\delta^{18}O$ series of three species (the correlation coefficient is shown in table thereinto) and their first principal component (PC1) (a), and comparision between the PC1 and observed summer $\delta^{18}O$ of precipitation in Zhangye (b) source from Global Network of Istopes in Precipitation project (http://www-naweb.iaea.org).

humidity reanalyzed from NCEP/NCAR data (NCEP/NCAR Reanalysis $RHUM_{sfc}$), CRU precipitation (CRU TS4.01 PRE), CRU cloud cover (CRU TS4.01 CLD), CRU drought index (CRU $_{SC}$PDSI), and sea-level pressure reanalyzed from NCEP/NCAR data (NCEP/NCAR Reanalysis SLP) provided by the Climate Research Unit (CRU) and NOAA/OAR/ESRL PSD from their Web site at https://www.cru.uea.ac.uk/ and https://www.esrl.noaa.gov/psd/ , respectively. The spatial correlograms were plotted using the software MATLAB 2015b. PC1 was compared with several East Asian Summer Monsoon indices, defined as follows. The Huang index is defined as the average zonal wind at 200 hPa pressure level in east Asia minus that in the equatorial region plus that in the subtropical and mid-latitude regions (Zhao et al., 2015). The Wang index is defined as the normalized zonal wind shear (or difference) between 850 hPa and 200 hPa averaged over 20° to 40° N and 110° to 140° E (Wang et al., 2008). The Li index is defined as an area-averaged seasonally (JJA) dynamical normalized seasonality at 850 hPa within the East Asian monsoon domain (10° to 40° N, 110° to 140° E) (Li and Zeng, 2002). The Zhu index was developed for land-sea between zonal and meridional thermal difference in terms of the East Asian zonal sea-level pressure contrast combined with high and low-level zonal wind shear at low latitudes (Zhu et al., 2000). The observed $\delta^{18}O$ of precipitation data source from the Global Network of Isotopes in Precipitation project (http://www-naweb.iaea.org). The El Nino Modoki index was obtained from the Japan Agency for Marine-Earth Science and Technology (http://www.jamstec.go.jp/).

3. Results and discussion

3.1. Tree-ring $\delta^{18}O$ series of the three species

High intra-species consistency was observed in the $\delta^{18}O$ series of the three species. The mean correlation coefficient (r_{mean} or R_{BAR}) was 0.726 ($p < 0.001$, $n = 30$) among the three $\delta^{18}O$ series of *H. rhamnoides* shrubs (Fig. 2a). The (r_{mean})of *P. euphratica* was 0.722 ($p < 0.001$, $n = 30$) (Fig. 2b), and (r_{mean}) of the *P. crassifolia* series was 0.700 ($p < 0.001$, $n = 30$) (Fig. 2c). The latter was relatively low compared to the other two species although the value was significant. This is probably due to the fact that the three samples of *P. crassifolia* were collected at different elevations.

The minimum number of trees for tree-ring isotopes studies is generally far few than that of ring width or density studies (Leavitt, 2010; Mccarroll and Loader, 2004). In some cases, two trees could even represent the common regional signal in tree-ring isotopes studies (Leavitt and Long, 1984; Li et al., 2011b; McCarroll and Pawellek, 1998; Robertson et al., 1997). Leavitt (2010) and Mccarroll and Loader (2004) suggested that the minimum number of trees should be calculated by the Expressed Population Signal (EPS). In this study, all EPSs of the tree-ring $\delta^{18}O$ series for three species were 0.99, higher than the guide threshold value of 0.85, above which one can infer that the averaged time-series represents the common regional signals (Wigley et al., 1984). These results suggest that the three trees are enough to reflect the species or regional signals in their sampling sites.

Because the $\delta^{18}O$ in individual samples of the same species were significantly correlated, we computed the average $\delta^{18}O$ series for each

of the species by averaging individual series from the same species (Fig. 2d). Within the common time interval, the average $\delta^{18}O$ value was the highest in the desert tree *P. euphratica* (35.2 ± 0.6 ‰). This is probably due to the fact that this species was growing in the most arid environment among the three sampling sites, and that the transpiration of its leaves is also the most pronounced. Therefore, a large quantity of the ^{16}O in the leaves quickly escapes and more ^{18}O remains. The average $\delta^{18}O$ value of *H. rhamnoides* was 33.9 ± 1.1 ‰, which was the lowest among the three species over the same time period. This could be attributed to the fact that this species was located in the Qilian Mountains at the edge of the Tibetan Plateau where precipitation is relatively abundant. In addition, the average $\delta^{18}O$ in *H. rhamnoides* was close to that in the *Juniperus chinensis* L. located on the northeastern Tibetan Plateau (Wang et al., 2013b). It is noteworthy that the differences between the average $\delta^{18}O$ values of the three species are not only caused by climatic factors, but also by physiological factors. For instance, the $\delta^{18}O$ exchange ratio between carbohydrates in the tree and tree trunk water may vary with species. And, diverse altitudes of the sampling sites result in different $\delta^{18}O$ values of precipitation (altitude effect), which may be another reason in species differences $\delta^{18}O$ of the three species in this study (Li et al., 2011c).

We normalized the average $\delta^{18}O$ series of the tree species (Fig. 3a) and found that their variations and extremes were basically consistent. For example, very low $\delta^{18}O$ values were observed in 1979 and 1993, while very high $\delta^{18}O$ values were found in 1982 and 1985. There was a significant correlation between the three series (Fig. 3a). The mean correlation coefficient of the three $\delta^{18}O$ series was 0.674 ($p < 0.001$, $n = 30$). The coherent variation is agreement with some similar studies of the world. For example, $\delta^{18}O$ series of six tree species of lowland in Bolivia show synchronous variation, which is most likely arising from similar trend of $\delta^{18}O$ in source water (Baker et al., 2015). In central Japan, coherent variations of $\delta^{18}O$ in pine and oak may result from same relative humidity (Li et al., 2015b). Those results suggested that within a same climate region, $\delta^{18}O$ variations of different trees may similar. The current study is unique due to including $\delta^{18}O$ of shrub, and large-scale (> 200 km) comparison. Principal component analysis was subsequently performed to extract the first principal components (PC1) of the three series.

3.2. The $\delta^{18}O$ in precipitation

Soil water is absorbed by the tree roots and transported to the leaves. After transpiration and photosynthesis, it is used to generate carbohydrates. The resulting carbohydrates are then transported to the stems of the trees to form cellulose that is fixed in the wood formed in the same year. Because cellulose is a polymer, its elements will not migrate once it is formed. This is why tree-ring cellulose $\delta^{18}O$ inherits the $\delta^{18}O$ signals from the soil water (Roden et al., 2000). The conifers commonly used in dendroclimatological research are generally shallow-rooted (Tubbs et al., 1987). They directly absorb the shallow soil water after precipitation. This is why in many cases; a strong relationship is observed between tree-ring $\delta^{18}O$ and precipitation $\delta^{18}O$. For example, tree-ring $\delta^{18}O$ in the *Quercus* from Lac d'Annecy, France (Danis et al., 2006), the *M. acantholoba* from southern Mexico (Brienen et al., 2013), the *Larix decidua* Sullivan from Italy (Leonelli et al., 2017), *Chamaecyparis formosensis* Matsumura in Taiwan (Liu et al., 2017a), *Larix principis-rupprechtii* from Luya Mountain in Shanxi, and the *Pinus tabuliformis* from Yaoshan Mountain in Henan (Liu et al., 2017b) were all found to be coherent with precipitation $\delta^{18}O$ variations recorded in the vicinity.

Hippophae . rhamnoides is a shallow-rooted plant, with a root depth ranging from 0 to 60 cm (Liu et al., 2005a). And *P. crassifolia* trees are also typically shallow-rooted plant (Li et al., 2019). In arid and semi-arid areas, there is less rainfall during the growing season (Wang et al., 2013a). Precipitation is hence absorbed quickly by shallow-root systems of plants The root system of *P. euphratica* is more developed and reaches several meters below the surface, which may tap groundwater (Rajput et al., 2016). However, the evidences of water chemistry and model analysis indicated that the groundwater was mainly sourced from precipitation in the sampling site of *P. euphratica* (Jiao et al., 2015; Su et al., 2010). Consequently, all the species in this study used precipitated water quite swiftly in theory.

In our study area, only a limited amount of observation data regarding precipitation $\delta^{18}O$ was available, with only ten years of observation in Zhangye. As shown in Fig. 3b, precipitation-amount-weighted $\delta^{18}O$ variation in summer precipitation and PC1 exhibited a coherent trend in the same direction. This suggests that tree-ring $\delta^{18}O$ in the region inherited the signal from precipitation $\delta^{18}O$. Nonetheless, the time period covered by the precipitation $\delta^{18}O$ record is too short to acquire further details and too short for reconstructing precipitation $\delta^{18}O$ from tree rings. Simulations of variations in local and regional precipitation $\delta^{18}O$ have been conducted by some researchers using various reanalyzed data owing to the importance of precipitation $\delta^{18}O$ (Vuille et al., 2003; Yoshimura et al., 2011). However, more independent indicators are required to validate the simulation results. On a global scale, only a small amount of observed precipitation $\delta^{18}O$ data recorded over a limited time period is available. Therefore, tree-ring $\delta^{18}O$ may be used for future validation and improvement of the results from precipitation $\delta^{18}O$ simulations, thereby enhancing the application of simulated precipitation $\delta^{18}O$ data in environmental isotope studies.

3.3. Climatic responses and spatial representative

The climatic responses demonstrated by the $\delta^{18}O$ series of the three species were similar to the meteorological observations in the vicinity (Fig. 4). Significant correlation with the spring-summer record of the current year was observed. On the other hand, they did not exhibit significant association with previous-year climatic factors in the growing season, indicating that the climatic conditions of the previous year did not exert a lagged effect on tree-ring $\delta^{18}O$ in the current year. In general, tree-ring $\delta^{18}O$ exhibited negative correlation with the present-year spring-summer RH and P, and a positive correlation with T (Liu et al., 2009; Roden et al., 2000; Saurer, 1997). This pattern is consistent with the climatic responses shown in tree-ring $\delta^{18}O$ in most parts of the world (Leavitt, 2010; Mccarroll and Loader, 2004; Sternberg, 2009; Treydte et al., 2007).

The negative correlation with RH is the most significant correlation observed in this study (Fig. 4). The correlation coefficient between *P. crassifolia* and the local June-August RH was determined to be −0.888 ($p < 0.001$, $n = 30$). The correlation coefficient between *P. euphratica* and July-August RH was found to be −0.75 ($p < 0.001$, $n = 30$), and that between *H. rhamnoides* and RH from July to August was −0.644 ($p < 0.001$, $n = 30$). This is agreement with previous studies proved that in addition to precipitation $\delta^{18}O$, RH is a key factor that controls tree-ring $\delta^{18}O$ (Leavitt, 2010; Mccarroll and Loader, 2004). The possible mechanism is assumed to be that the leaf-to-air vapor pressure ratio is approximately equal to RH (Mccarroll and Loader, 2004).

Although temperature is not the dominant environmental signals in tree-ring $\delta^{18}O$, theoretically (Mccarroll and Loader, 2004), there are two possible reasons for the significant positive correlation with temperature in this study (Fig.4). First, the tree-ring $\delta^{18}O$ inherits $\delta^{18}O$ of precipitation in this study (Fig. 3b). It is generally that precipitation $\delta^{18}O$ shows positive correlation with the local temperature in inland areas such as the sampling site that are far from the sea (temperature effect) (Dansgaard, 1964). Second, $\delta^{18}O$ of the leaf water is modified by evaporation which depends on stomatal conductance and vapor pressure deficit, while both of stomatal conductance and vapor pressure deficit are linked with RH in theory (Mccarroll and Loader, 2004; Roden et al., 2000; Sternberg, 2009). Therefore, there is a significant negative correlation between RH and tree-ring $\delta^{18}O$, agreeing with Fig. 4 in this study. The temperature and RH are negatively correlated in the study area (Li et al., 2019), resulting in a significant positive

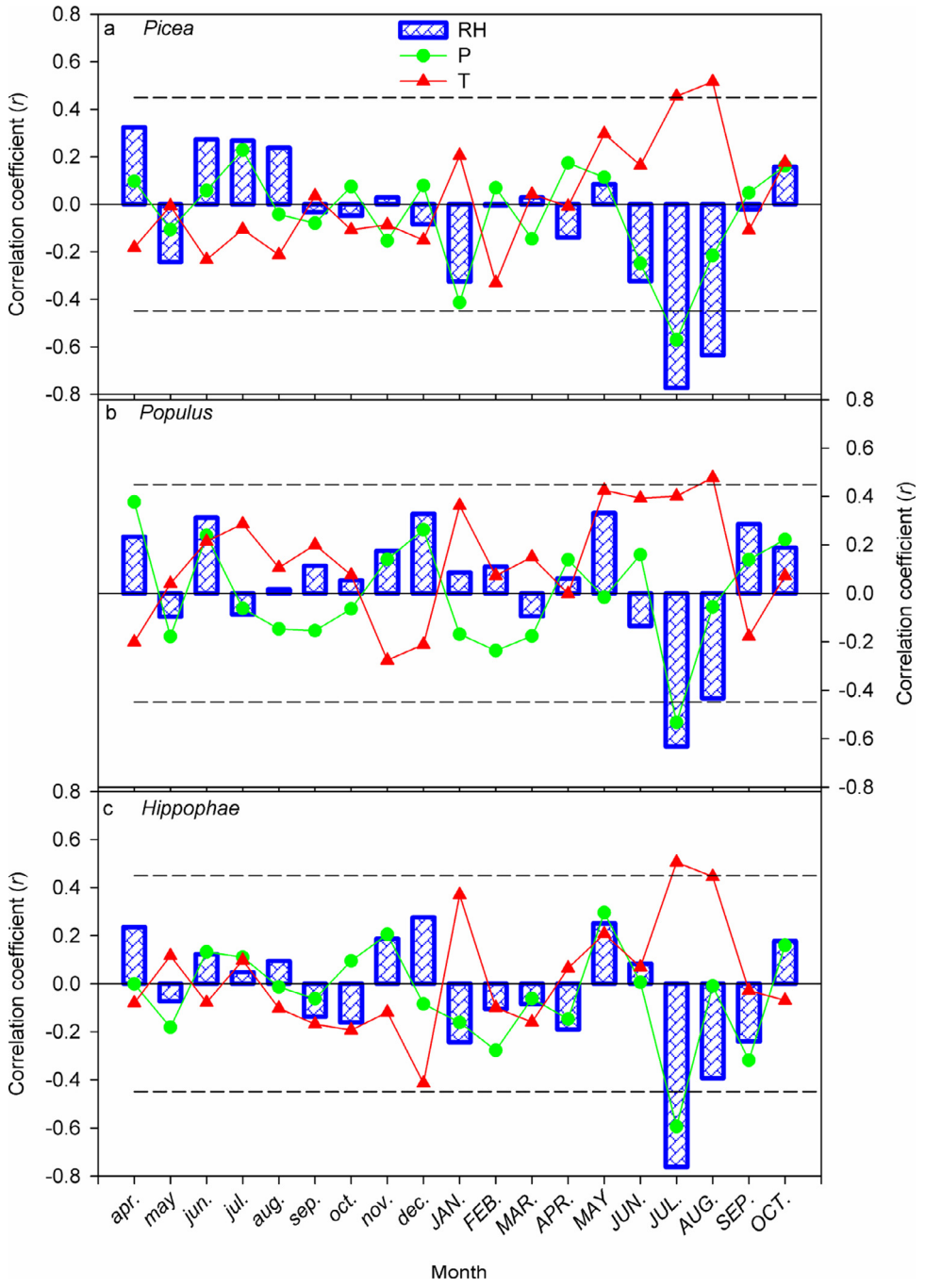

Fig. 4. The correlation coefficients between instrumental relative humidity (RH), precipitation (P), temperature (T) and mean $\delta^{18}O$ series of *P. crassifolia*(a), *P. euphratica* (b), and *H. rhamnoides* (c) during previous April to current October.

correlation between the temperature and tree-ring $\delta^{18}O$. Because there is a significant positive correlation between the observed precipitation and RH in the area, the spring-summer precipitation exhibits a significant negative correlation with tree-ring $\delta^{18}O$.

Despite the great distance and the remarkable differences in site conditions between the three species, their $\delta^{18}O$ variations were found to be consistent. The main reason is that the RH variations at the three sites were basically coherent. As shown in Fig. 5a, the trends of the observed RH values recorded near each of the three sampling sites from June to August were almost equivalent: the average correlation coefficient of the three RH curves was found to be 0.732 ($p < 0.001$, $n = 30$). However, there was a significant difference between the absolute values of RH at the three sites. The lowest RH (34%) was recorded in the area where *P. euphratica* was located, while the highest RH was recorded at the area where *H. rhamnoides* was located (48%). RH is defined as the ratio of the vapor pressure to the saturated vapor pressure of water at a given temperature, and the multi-year average temperatures of the three sites were similar. We may therefore estimate that the differences between dry and wet environments were characterized by the variations in RH. Hence, as shown in Fig. 5a, the environment where *P. euphratica* grows is the most arid environment, leading to the highest average $\delta^{18}O$ value being recorded in this species. The environment where *H. rhamnoides* grows is more humid, and hence exhibits the lowest average $\delta^{18}O$ value (Fig. 2d).

We extracted the regionally monthly RH, precipitation, and temperature variations from records of the all meteorological stations over

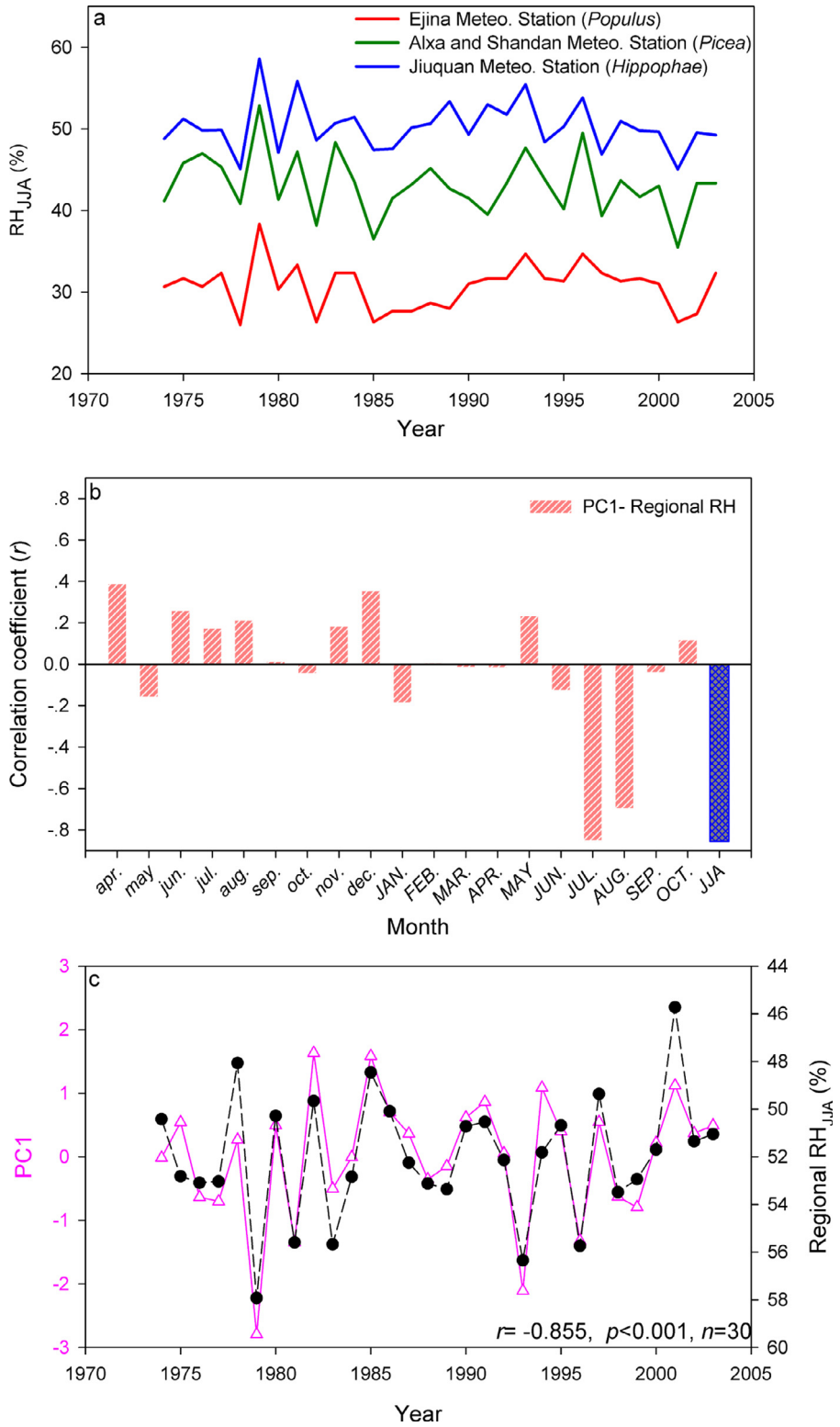

Fig. 5. Summer (June to August) RH variations recorded by nearby meteorological stations of three species (a), the correlation coefficients between regional RH and the PC1 during previous April to current October (b), and comparision between the PC1 and regional summer RH (c).

the area of 38° to 42° N, 97° to 102° E by spatial interpolation using MATLAB 2015b. PC1 showed the highest correlation with the regional June-August RH ($= -0.855, p < 0.001, n = 30$), explaining 73.1% of the variance in the observed RH (Fig. 5b and 5c). The correlation coefficient between PC1 and the regional June-August precipitation was found to be -0.783 ($p < 0.001$, $n = 30$). The correlation between PC1 and temperature is the lowest, with a maximum value of only 0.484 in the months of July to August. The highest correlation with RH is best explained by the physiological mechanism. Because the RH is theoretically related to the leaf-to-air vapor pressure ratio (Mccarroll and Loader, 2004), which is one of the factors directly controlling tree-ring $\delta^{18}O$, PC1 and the regional summer RH variations were basically consistent over the past 30 years (Fig. 5c). Considering the mutual linkage between RH, precipitation, and temperature, we

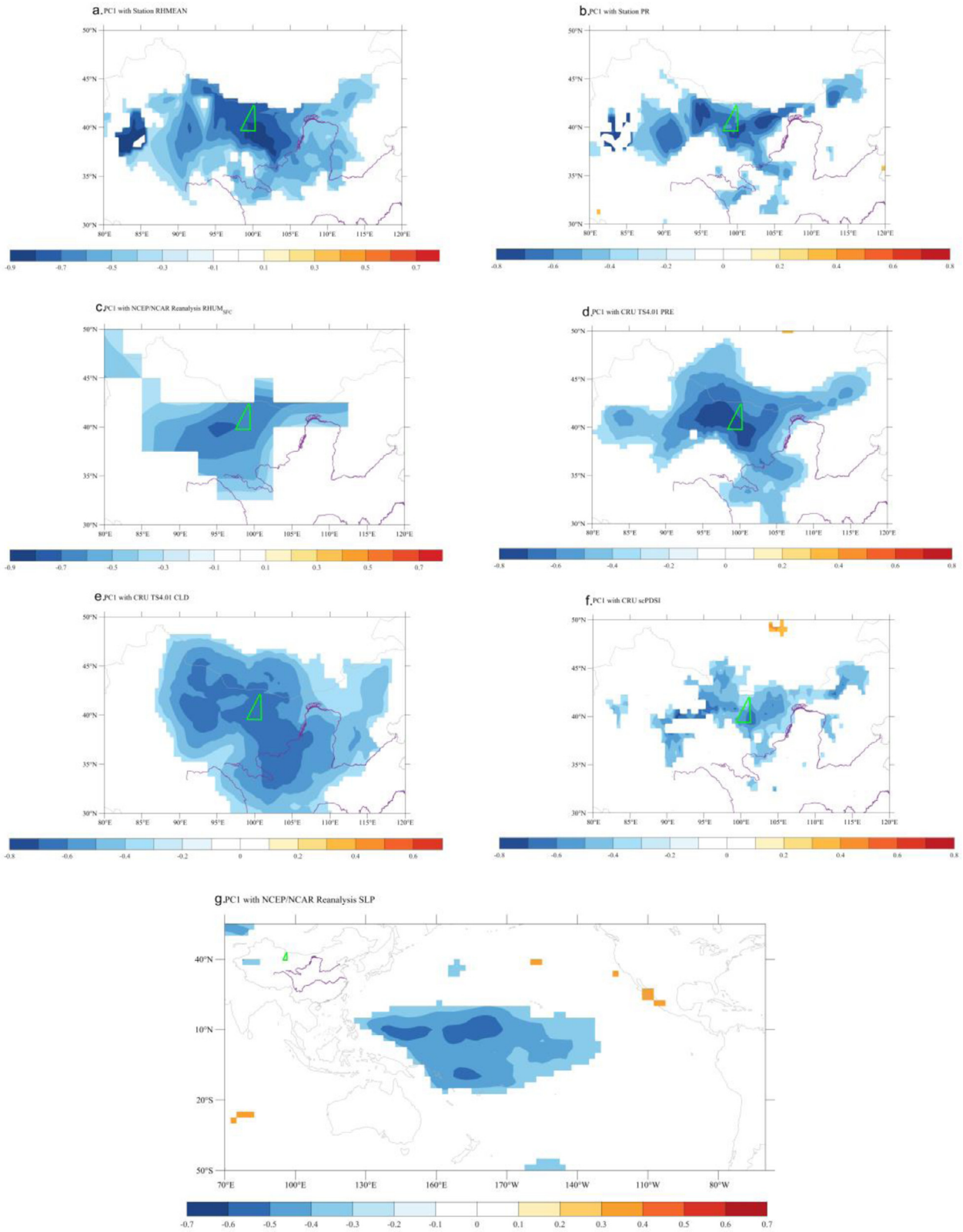

Fig. 6. Spatial correlation patterns between the PC1 and several hydroclimate-related globally gridded datasets. The details of globally gridded datasets are descriped in Section 2.3.

analyzed the partial correlations between the tree-ring $\delta^{18}O$ and regional June-August RH, precipitation, and temperature in order to summarize the effect of primary climatic factor on tree-ring $\delta^{18}O$. The results show that when temperature is controlled, there is still a notable correlations between the tree-ring $\delta^{18}O$ and RH ($r = -0.826$, $p < 0.001$, $n = 30$), and between the tree-ring $\delta^{18}O$ and precipitation ($r = -0.738$, $p < 0.001$, $n = 30$); but when RH is controlled, the correlation coefficient between the tree-ring $\delta^{18}O$ and temperature, and

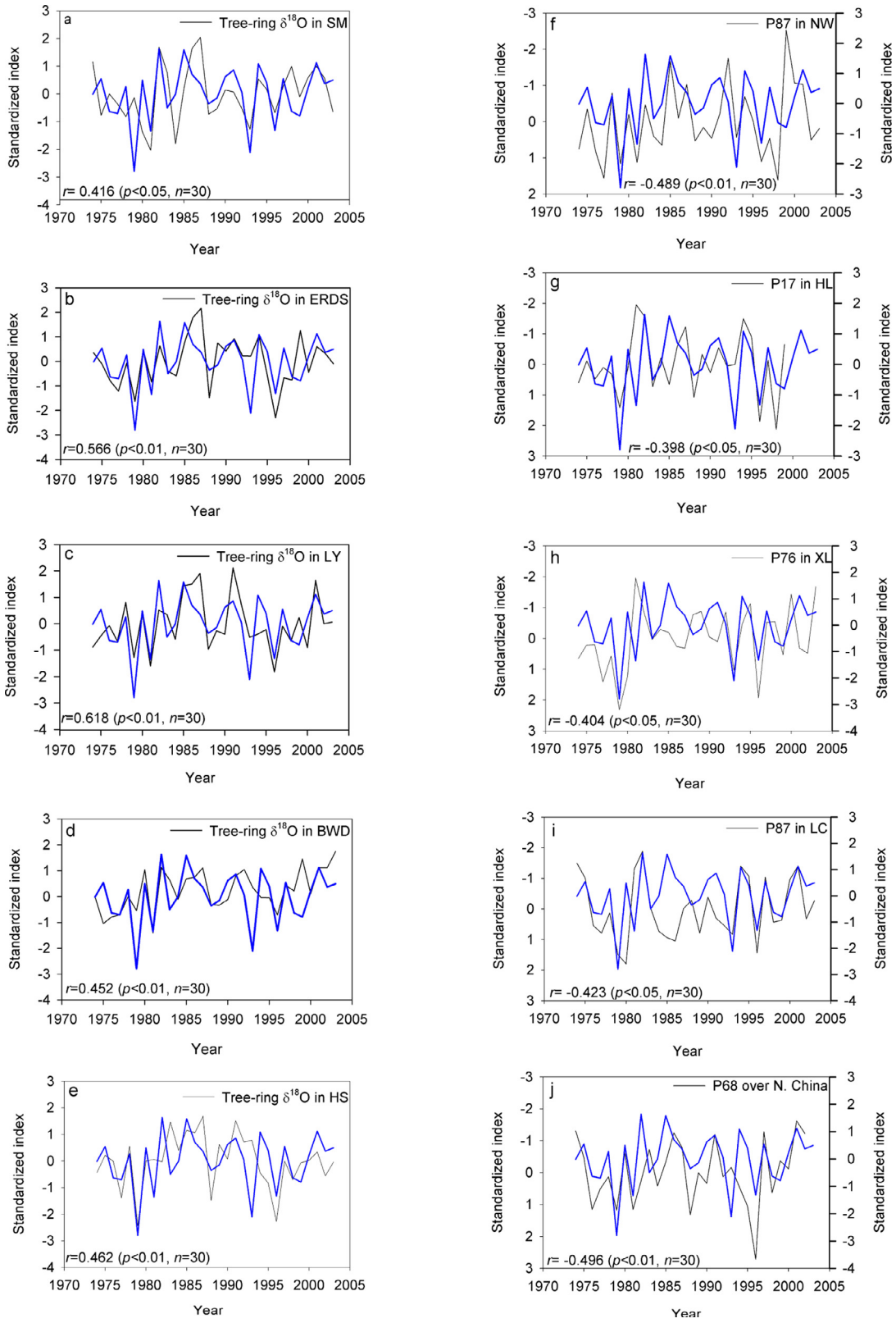

Fig. 7. The comparison between the PC1 and the tree-ring $\delta^{18}O$ variations in Shimen Mountain, Gansu Province (SM, a), Ordos Plateau, Inner Mongolia (ERDS, b), Luya Mountain, Shanxi Province (LY, c), Beiwudang Mountain (BWD, d), Hengshan Mountain (HS,e), reconstructed previous August to current July precipitation (P87) in Ningwu (f), reconstructed January to July precipitation (P17) in Helan Mountain (g), reconstructed previous July to current June precipitation (P76) in Xinglong Mountain (h), reconstructed previous August to current July precipitation (P87) in Liancheng (i) and reconstructed June to August precipitation (P68) over North China (j). The correlation coefficient is shown in figures. The locations of above reconstructions are indicated in Fig.1a.

between the tree-ring $\delta^{18}O$ and precipitation are only −0.087 and −0.128, respectively. Hence, we suggest that the July-August temperature and PC1 ($r = 0.484$) are indirectly correlated. The primary climatic factor that controls the tree-ring $\delta^{18}O$ is RH.

The above analyses indicated that the major climatic factors controlling PC1 are the regional RH and precipitation. To examine the spatial extent to which PC1 could represent the hydroclimatic variations, we performed spatial correlation analyses on PC1 and the hydroclimatic spatial grid-point datasets with global coverage (Fig. 6). We found that PC1 represents hydroclimatic variations at a broad-scale that covers approximately central-western China. It is noteworthy that there are negative correlations between PC1 and all hydroclimatic parameters in Fig. 6, which can be explained by the fact that tree-ring $\delta^{18}O$ is negatively correlated with RH and precipitation due to physiological processes. Despite the significant correlation with PDSI, we can see that the area involved is smaller. This may be attributed to the close association of PDSI with temperature, which exerts only slight influence on tree-ring $\delta^{18}O$. In addition, we recognized a significant negative correlation between PC1 and the sea-level pressure in the central Pacific (Fig. 6g). As the sea-level pressure in the Pacific increases, the wind direction changes to blow from the ocean onto the Asian continent. Therefore, a large amount of water vapor is transported by the wind to central-western China, resulting in a rise in the regional humidity and a decline in tree-ring $\delta^{18}O$. We already knew that the East Asian Summer Monsoon (EASM), which affects most parts of China, is mainly caused by the land-sea thermal contrast closely related to the changes in sea-level pressure (Zhao et al., 2015; Zhu et al., 2000). Consequently, Fig. 6g also implies that the regional tree-ring $\delta^{18}O$ in our study could be associated with the EASM on a large spatial-temporal scale. By comparing PC1 with several well-known EASM indices, we found that PC1 is significantly correlated with these EASM indices as defined by various authors. For example, the correlation coefficients between PC1 and Huang index (Zhao et al., 2015), Wang index (Wang et al., 2008), Li index (Li and Zeng, 2000) and Zhu index (Zhu et al., 2000) are −0.516 ($p < 0.01$), −0.502 ($p < 0.01$), 0.498 ($p < 0.01$) and 0.416 ($p < 0.05$), respectively. This confirms that tree-ring $\delta^{18}O$ can be used as an indicator of the EASM moisture in our study area. In areas with strong effects from the EASM, the hydroclimatic variations should, theoretically, synchronize with PC1. This is verified in Fig. 6 by the spatial correlation of PC1 with the observed hydroclimatic parameters.

3.4. Potential for establishing a hydroclimate network

During the growth of trees, they are normally affected by factors such as the growth trends and competition between individuals in the forest. To eliminate the effect of these non-climatic factors, the first step of establishing chronologies based on tree-ring width or density is to remove these non-climatic signals using a negative exponential or linear function. However, low-frequency climatic signals would be removed at the same time. Tree-ring $\delta^{18}O$ represents the ratio between ^{18}O and ^{16}O, and is independent of growth. Consequently, detrending is not required when establishing tree-ring $\delta^{18}O$ chronologies. Because the results from Isotope Ratio Mass Spectrometry are directly used for climatic analysis, both high- and low-frequency climatic signals are retained. This is also the significant difference between tree-ring $\delta^{18}O$ and common biological indicators.

In order to examine the potential of the tree-ring $\delta^{18}O$ series that was synthesized from shrubs, broad-leaved trees, and conifer trees to establish a broader-scale climate change network (along with the other hydroclimatic series reconstructed from tree-rings in central-western China), we compared PC1 with a total of ten tree-ring indices and tree-ring-based reconstructions from central-western China. These included four tree-ring $\delta^{18}O$ series established in this study (Shimen Mountain, Gansu Province; Ordos Plateau, Inner Mongolia; Beiwudang Mountain, Shanxi Province; and Hengshan Mountain, Shanxi Province), a published tree-ring $\delta^{18}O$ series (Luya Mountain), and five published reconstructed precipitation series (based on tree-ring width). These study sites are all located in regions that experience notable influence from the EASM (Fig. 1a). The result of the comparison is illustrated in Fig. 7. The resulting correlation coefficients are all significant ($p < 0.05$). The series are basically consistent with the variations in PC1. The highest correlation coefficient found was with the tree-ring $\delta^{18}O$ series of *Larix principis-rupprechtii* from the Luya Mountain in Shanxi (Fig.7c), which was determined to be 0.618 ($p < 0.01$, $n = 30$). The tree-ring $\delta^{18}O$ series in the Luya Mountain share notable characteristics with the EASM variabilities and is thus a good indicator of EASM precipitation (Li et al., 2011a). The weakest correlation was with the reconstructed January-July precipitation in the Helan Mountains (Fig. 7g), with a correlation coefficient of 0.398 ($p < 0.05$, $n = 30$). The reason for the slightly lower correlation coefficient might be due to the fact that the reconstructed precipitation in the Helan Mountains also included winter-spring climatic signals (Liu et al., 2005b).

Moreover, we observed an interesting phenomenon: almost all of the time series in Fig. 7 indicated that 1979 was an extremely humid year. In fact, meteorologists have found that an abrupt climate change occurred in 1979 based on observational records. The summer-season precipitation in the entire eastern part of China increased gradually in 1979. The summer precipitation increased by nearly 100 mm in 1980–1999 compared to that in 1957–1979. This might have been caused by change in the sea-surface temperature (SST) in the eastern Pacific (Gong and Ho, 2002). As a result, after 1980, the western North Pacific subtropical high was intensified and migrated towards the southwest, changing the direction of water vapor transport (Zhou et al., 2009). In general, whether the SST of the central and eastern equatorial Pacific increases (El Nino) or decreases (La Nina), there is only one complete Walker circulation in the equatorial Pacific atmosphere-ocean system. Some scholars believe that after the 1970s, the mode of ENSO changed (Weng et al., 2007). Due to the notable increase of SST in the Central Pacific, the original atmosphere-ocean circulation pattern over the Pacific Ocean was interrupted and became two independent atmosphere-ocean circulation modes (i.e., the El Nino Modoki or the Central Pacific ENSO mode) (Takahashi et al., 2011). Some scholars believe that the El Nino Modoki was strengthened due to global warming caused by increased human activities (Yeh et al., 2009). After 1979 (i.e., 1980–2003), the variations in PC1 and the El Nino Modoki index were coherent ($r = 0.473$, $p < 0.02$, $n = 24$), indicating that, although the sampling sites are located in western China, tree-ring $\delta^{18}O$ is still sensitive to abrupt regime shifts such as the El Nino Modoki events (Fig. 8).

Single-site climate reconstruction does not reflect abrupt regional climate changes. More pre-instrumental broad-scale abrupt climate change events could be discovered if we integrated long time-scale records using multiple plant species that grow under different site conditions to reconstruct a high-resolution regional hydroclimatic record. These may offer important insights for the understanding of historical events (such as alternation of dynasties) that might be related to natural variabilities, the background of extreme climates, and their mechanisms.

4. Conclusions

This study is the first attempt to compare the annual-ring $\delta^{18}O$ variations of shrubs growing close to glaciers, conifer trees growing in alpine meadow and broad-leaves trees growing in desert oasis. Not only was the intra-species annual-ring $\delta^{18}O$ consistent, the variations in the averaged $\delta^{18}O$ series were remarkably coherent among these three species. Two are the main reasons for the coherence in $\delta^{18}O$ variation among the three species. The first is that they all inherited $\delta^{18}O$ signals from the regional precipitation, and the other is that the RH variations at the three sampling sites were similar.

The $\delta^{18}O$ in the three species were found to be significantly negatively correlated with the spring-summer RH and P, and positively

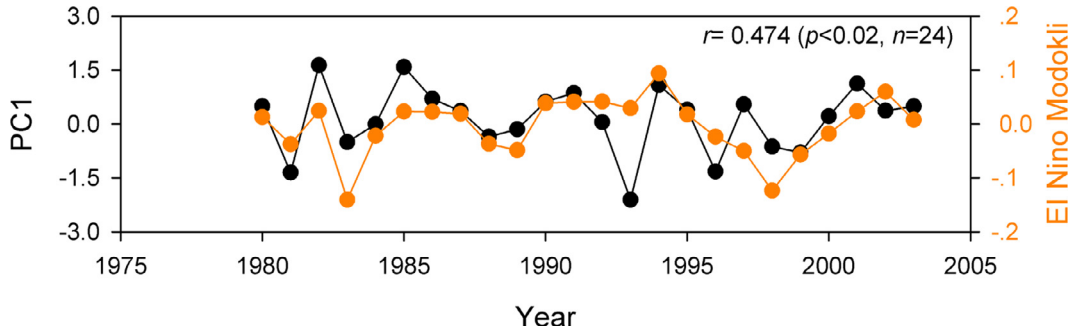

Fig. 8. Comparison between the PC1 and summer EI Nino Modoki index.

correlated with the T. The correlation coefficient between the first principal component of the three $\delta^{18}O$ series (PC1) and the regional summer (JJA) RH was found to be -0.855 ($p < 0.001$, $n = 30$). The variations in PC1 were found to be consistent with those of ten tree-ring indices/reconstructions for central-western China. Further, the spatial correlation revealed that the PC1 could represent the hydroclimatic variations in most areas of central-western China, demonstrating the potential benefit from establishing evenly distributed high-resolution paleoclimate network using annual-ring $\delta^{18}O$ of multiple plants. Especially, annual-ring $\delta^{18}O$ of shrub may become a powerful proxy in filling gaps in high-resolution paleoclimate network because of its widely distribution.

The PC1 is significantly correlated with several EASM indices and with the Pacific sea-level pressure. This indicates that the tree-ring $\delta^{18}O$ is influenced by large-scale atmospheric circulation patterns. In addition, an abrupt climate change occurred in 1979 detected from the PC1 variations. After 1979, the PC1 varied coherently with the summer El Nino Modoki, revealing the sensitivity of the regional tree-ring $\delta^{18}O$ variation in capturing conditions over the remote ocean.

Declaration of Competing Interest

The authors declare that they have no known competing financial interests or personal relationships that could have appeared to influence the work reported in this paper.

Acknowledgments

This study was financially supported by grants from the National Natural Science Foundation of China (41873021, U1803245 and 41991251); the Youth Innovation Promotion Association of CAS (No. 2017451); the West Light Foundation of CAS, Young Star of Science and Technology, Shaanxi Province; the STEP program (Grant No. 2019QZKK0101) and the Cultivating Foundation of SKLLQG. This work is a contribution of The Belt and Road Center of Environmental Studies, the Institute of Earth and Environment, Chinese Academy of Sciences.

Supplementary materials

Supplementary material associated with this article can be found, in the online version, at doi:10.1016/j.agrformet.2020.107929.

References

Baker, J.C.A., et al., 2015. Oxygen isotopes in tree rings show good coherence between species and sites in Bolivia. Global Planetary Change 133, 298–308.
Brienen, R.J.W., Hietz, P., Wanek, W., Gloor, M., 2013. Oxygen isotopes in tree rings record variation in precipitation $\delta^{18}O$ and amount effects in the south of Mexico. J. Geophys. Res. Biogeosci. 118 (4), 1604–1615.
Briffa, K.R., Jones, P.D., Schweingruber, F.H., Karlén, W., Shiyatov, S.G., 1996. Tree-ring variables as proxy-climate indicators: problems with low-frequency signals. Climatic Variations and Forcing Mechanisms of the Last 2000 Years 41 Springer, Berlin, Heidelberg.
Browicz, K., 1977. Chorology of Populus euphratica Olivier. Arboretum Kornickie 22, 5–27.
Cook, E.R., et al., 2010a. Asian monsoon failure and megadrought during the last millennium. Science 328 (5977), 486.
Cook, E.R., et al., 2010b. Megadroughts in North America: placing IPCC projections of hydroclimatic change in a long-term palaeoclimate context. J. Quater. Sc. 25 (1), 48–61.
Danis, et al., 2006. Reconstruction of past precipitation $\delta^{18}O$ using tree-ring cellulose $\delta^{18}O$ and $\delta^{13}C$: a calibration study near Lac d'Annecy, France. Earth Planetary Sc. Lett. 243 (3), 439–448.
Dansgaard, W., 1964. Stable isotopes in precipitation. Tellus 16 (4), 436–468.
Davi, N., et al., 2010. Reconstructing drought variability for Mongolia based on a large-scale tree ring network: 1520–1993. J. Geophys. Res. 115 (D22).
Frank, D., Esper, J., 2005. Characterization and climate response patterns of a high-elevation, multi-species tree-ring network in the European Alps. Dendrochronologia 22 (2), 107–121.
Gong, D.Y., Ho, C.H., 2002. Shift in the summer rainfall over the Yangtze River valley in the late 1970s. Geophys Res Lett 29 (10), 71–78.
Grissino-Mayer, H.D., 1993. An updated list of species used in tree-ring research. Tree-ring bulletin 53, 17–43.
Jiao, J.J., Zhang, X., Wang, X., 2015. Satellite-based estimates of groundwater depletion in the Badain Jaran Desert. China. Sci. Rep. 5 (1), 8960.
Kagawa, A., Leavitt, S.W., 2010. Stable carbon isotopes of tree rings as a tool to pinpoint the geographic origin of timber. J. Wood Sci. 56 (3), 175–183.
Lawrence, A., Hawthorne, W., 2006. Plant identification: creating user-friendly guides for biodiversity management. Int. Foresty Rev. 2, 687–688.
Leavitt, S.W., 2010. Tree-ring C-H-O isotope variability and sampling. Sci. Total Environ. 408 (22), 5244.
Leavitt, S.W., Long, A., 1984. Sampling strategy for stable carbon isotope analysis of tree rings in pine. Nature 145–147.
Leavitt, S.W., Long, A., Dean, J.S., 1985. Tree-ring dating through pattern-matching of stable-carbon isotope time series. Tree-Ring Bulletin 45.
Leonelli, G., et al., 2017. Larix decidua $\delta^{18}O$ tree-ring cellulose mainly reflects the isotopic signature of winter snow in a high-altitude glacial valley of the European Alps. Sci. Total Environ. 579, 230–237.
Li, J., Zeng, Q., 2002. A unified monsoon index. Geophys Res Lett 29 (8) 115-1-115-4.
Li, Q., et al., 2019. East Asian summer monsoon moisture sustains summer relative humidity in the southwestern Gobi Desert, China: evidence from $\delta^{18}O$ of tree rings. Clim. Dyn. 52, 6321–6337.
Li, Q., et al., 2017. Climate responses of tree-ring stable oxygen isotopes from Yadong County, Tibetan Plateau. J. Earth Environ. 8 (1), 6–14.
Li, Q., Liu, Y., Song, H., Yang, Y., Zhao, B., 2015a. Divergence of tree-ring-based drought reconstruction between the individual sampling site and the Monsoon Asia Drought Atlas: an example from Guancen Mountain. Sci. Bull. 60 (19), 1688–1697.
Li, Q., Nakatsuka, T., Kawamura, K., Liu, Y., Song, H., 2011a. Hydroclimate variability in the North China Plain and its link with El Niño–Southern Oscillation since 1784 AD: insights from tree-ring cellulose δ18O. J. Geophys. Res. 116 (D22), 1984–2012.
Li, Q., Nakatsuka, T., Kawamura, K., Liu, Y., Song, H., 2011b. Hydroclimate variability in the North China Plain and its link with El Niño–Southern Oscillation since 1784 AD: insights from tree-ring cellulose $\delta^{18}O$. J. Geophys. Res 116, D22106.
Li, Q., Nakatsuka, T., Kawamura, K., Liu, Y., Song, H., 2011c. Regional hydroclimate and precipitation $\delta^{18}O$ revealed in tree-ring cellulose $\delta^{18}o$ from different tree species in semi-arid Northern China. Chem. Geol. 282 (1–2), 19–28.
Li, Z., Nakatsuka, T., Sano, M., 2015b. Tree-ring cellulose $\delta^{18}O$ variability in pine and oak and its potential to reconstruct precipitation and relative humidity in central Japan. Geochem J 49 (2), 125–137.
Liu, H.Z., Qi, J., Li, Y., 2005a. Studies on Seabuckthorn root fidtribution and rood dules. J. Jilun Agricult. University 27 (6), 631–636.
Liu, X., et al., 2009. Climatic significance of tree-ring $\delta^{18}O$ in the Qilian Mountains, northwestern China and its relationship to atmospheric circulation patterns. Chem. Geol. 268 (1–2), 147–154.
Liu, Y., et al., 2005b. Seasonal precipitation in the south-central Helan Mountain region, China. Can. J. For. Res. 35 (10), 2403–2412.
Liu, Y., et al., 2017a. Recent enhancement of central Pacific El Niño variability relative to last eight centuries. Nat Commun 8, 15386.
Liu, Y., et al., 2017b. A monsoon-related 174-year relative humidity record from tree-ring δ 18 o in the Yaoshan region, eastern central China. Sci. Total Environ. 593–594,

523–534 s.
Liu, Y., et al., 2010. Tree-ring hydrologic reconstructions for the Heihe River watershed, western China since AD 1430. Water Res. 44 (9), 2781–2792.
Liu, Y., Xie, L., Qiang, L.I., Cai, Q.F., 2012. Growth-climate response analysis between tree-ring width and March-September mean minimum temperature in Dongda Mountain,Gansu,China since 1820 Ad. J. Earth Environ. 3, 900–907.
Loader, N.J., et al., 2019. Tree ring dating using oxygen isotopes: a master chronology for central England. J. Quater. Sci. 34 (6), 475–490.
Loader, N.J., Robertson, I., Barker, A.C., Switsur, V.R., Waterhouse, J.S., 1997. An improved technique for the batch processing of small wholewood samples to α-cellulose. Chem. Geol. 136 (3), 313–317.
Mccarroll, D., Loader, N.J., 2004. Stable isotopes in tree rings. Quat. Sci. Rev. 23 (7), 771–801.
McCarroll, D., Pawellek, F., 1998. Stable carbon isotope ratios of latewood cellulose in Pinus sylvestris from northern Finland: variability and signal-strength. The Holocene 8 (6), 675.
Miles, D., et al., 2019. . stable isotope dating of historic buildings. J. Vernacular Architect. 1–10.
Palmer, J.G., et al., 2015. . Drought variability in the eastern Australia and New Zealand summer drought atlas (ANZDA, CE 1500–2012) modulated by the Interdecadal Pacific Oscillation. Environ. Res. Lett. 10 (12), 124002.
Rajput, V.D., et al., 2016. . a review on salinity adaptation mechanism and characteristics of Populus euphratica, a boon for arid ecosystems. Acta Ecológica Sinica 36 (6), 497–503.
Robertson, I., Rolfe, J., Switsur, V.R., Carter, A.H.C., Waterhouse, J.S., 1997. Signal strength and climate relationships in 13C/12C ratios of tree ring cellulose from oak in Southwest Finland. Geophys. Res. Lett. 24, 1487–1490.
Roden, J., 2008. Cross-dating of tree ring δ18O and δ13C time series. Chem. Geol. 252 (1–2), 72–79.
Roden, J.S., Lin, G., Ehleringer, J.R., 2000. A mechanistic model for interpretation of hydrogen and oxygen isotope ratios in tree-ring cellulose. Geochim. Cosmochim. Acta 64 (1), 21–35.
Saurer, M., 1997. δ^{18}O of tree eings of beech as a record of d18O of the growing season precipitation. Tellus 49B, 80–92.
Song, X., Clark, K.S., Helliker, B.R., 2014. Interpreting species-specific variation in tree-ring oxygen isotope ratios among three temperate forest trees. Plant Cell Environ. 37 (9), 2169–2182.
Sternberg, L.d.S.L.O.R., 2009. Oxygen stable isotope ratios of tree-ring cellulose: the next phase of understanding. New Phytol. 181.
Su, Y., et al., 2010. Characterization of groundwater in the Ejina Basin,Northwest China: hydrochemical and environmental isotopes approaches. Sci. Cold Arid Regions 2 (6), 0477–0497.
Takahashi, K., Montecinos, A., Goubanova, K., Dewitte, B., 2011. ENSO regimes: reinterpreting the canonical and Modoki El Niño. Geophys. Res. Lett. 38 (10), L10707.
Tang, S., et al., 2013. Populus euphratica: the transcriptomic response to drought stress. Plant Mol. Biol. 83 (6), 539–557.
Treydte, K., et al., 2007. Signal strength and climate calibration of a European tree-ring isotope network. Geophys Res Lett. 34 (24).
Tubbs, C.H., DeGraaf, R.M., Yamasaki, M., Healy, W.M.J.G.T.R.N.-B., 1987. PA: US department of agriculture, forest service, northeastern forest experiment station. 30 p. Guide to wildlife tree management in New England northern hardwoods 118, 1–30.
Vuille, M., et al., 2003. Modeling δ^{18}O in precipitation over the tropical Americas: 2. simulation of the stable isotope signal in Andean ice cores. J. Geophys. Res. 108 (D6).
Wang, B., Wu, Z., Li, J., Jian, L., Wu, G., 2008. How to measure the strength of the East Asian summer monsoon. J. Clim. 21 (17), 4449–4463.
Wang, H., Chen, Y., Chen, Z., 2013a. Spatial distribution and temporal trends of mean precipitation and extremes in the arid region, northwest of China, during 1960–2010. Hydrol. Process. 27, 1807–1818.
Wang, W.Z., et al., 2013b. Moisture variations over the past millennium characterized by Qaidam Basin tree-ring δ ^{18}O. Chin. Sci. Bull. 58 (32), 3956–3961.
Weng, H., Ashok, K., Behera, S.K., Rao, S.A., Yamagata, T., 2007. Impacts of recent El Niño Modoki on dry/wet conditions in the Pacific rim during boreal summer. Clim. Dyn. 29 (2–3), 113–129.
Wigley, T.M.L., Briffa, K.R., Jones, P.D., 1984. On the average value of correlated time series, with applications in dendroclimatology and hydrometeorology. J. Climatol. Appl. Meteorol. 23 (2), 201–213.
Yang, F., et al., 2013. Comparison of the dryness/wetness index in China with the Monsoon Asia Drought Atlas. Theoretical Appl. Climatol. 114 (3–4), 553–566.
Yeh, S.W., et al., 2009. El nino in a changing climate. Nature 462 (7263), 674.
Yoshimura, K., et al., 2011. Comparison of an isotopic AGCM with new quasi global satellite measurements of water vapor isotopologues. J. Geophys. Res. Atm. 116 (D19).
Zhao, G., et al., 2015. A new upper-level circulation index for the East Asian summer monsoon variability. J. Clim. 28 (24), 9977–9996.
Zhou, T.J., et al., 2009. Why the western pacific subtropical high has extended westward since the late. J. Clim. 22 (8), 2199–2215.
Zhu, C., He, J., Wu, G., 2000. East Asian monsoon index and its interannual relationship with largescale thermal dynamic circulation. Acta Meteorol. Sinica 58 (4), 391–402.
Zhu, H., Xu, P., Shao, X., Luo, H., 2013. Little Ice Age glacier fluctuations reconstructed for the southeastern Tibetan Plateau using tree rings. Quat. Int. 283 (Complete), 134–138.